

Electrospinning Core-Shell Nanofibers for Interfacial Toughening and Self-Healing of Carbon-Fiber/Epoxy Composites

Xiang-Fa Wu,¹ Arifur Rahman,¹ Zhengping Zhou,¹ David D. Pelot,² Suman Sinha-Ray,² Bin Chen,^{3,4} Scott Payne,⁵ Alexander L. Yarin²

¹Department of Mechanical Engineering, North Dakota State University, Fargo, North Dakota 58108-6050

²Department of Mechanical and Industrial Engineering, University of Illinois-Chicago, Chicago, Illinois 60607-7022

³Advanced Studies Laboratory, NASA Ames Research Center, Moffett Field, California 94035

⁴Baskin School of Engineering, University of California, Santa Cruz, California 95064

⁵Electron Microscopy Center, North Dakota State University, Fargo, North Dakota 58108-6050

Correspondence to: X.-F. Wu (E-mail: xiangfa.wu@ndsu.edu) or A. L. Yarin (E-mail: ayarin@uic.edu)

ABSTRACT: This article reports a novel hybrid multiscale carbon-fiber/epoxy composite reinforced with self-healing core-shell nanofibers at interfaces. The ultrathin self-healing fibers were fabricated by means of coelectrospinning, in which liquid dicyclopentadiene (DCPD) as the healing agent was enwrapped into polyacrylonitrile (PAN) to form core-shell DCPD/PAN nanofibers. These core-shell nanofibers were incorporated at interfaces of neighboring carbon-fiber fabrics prior to resin infusion and formed into ultrathin self-healing interlayers after resin infusion and curing. The core-shell DCPD/PAN fibers are expected to function to self-repair the interfacial damages in composite laminates, e.g., delamination. Wet layup, followed by vacuum-assisted resin transfer molding (VARTM) technique, was used to process the proof-of-concept hybrid multiscale self-healing composite. Three-point bending test was utilized to evaluate the self-healing effect of the core-shell nanofibers on the flexural stiffness of the composite laminate after predamage failure. Experimental results indicate that the flexural stiffness of such novel self-healing composite after predamage failure can be completely recovered by the self-healing nanofiber interlayers. Scanning electron microscope (SEM) was utilized for fractographical analysis of the failed samples. SEM micrographs clearly evidenced the release of healing agent at laminate interfaces and the toughening and self-healing mechanisms of the core-shell nanofibers. This study expects a family of novel high-strength, lightweight structural polymer composites with self-healing function for potential use in aerospace and aeronautical structures, sports utilities, etc. © 2012 Wiley Periodicals, Inc. *J. Appl. Polym. Sci.* 129: 1383–1393, 2013

KEYWORDS: electrospinning; fibers; mechanical properties; nanostructured polymers

Received 20 October 2012; accepted 8 November 2012; published online 10 December 2012

DOI: 10.1002/app.38838

INTRODUCTION

After over four-decade intensive research, advanced composites made of high-modulus fibers in compliant polymeric matrix have emerged as lightweight structural materials of the choice for many aerospace and aeronautical applications because of their distinct advantages superior to traditional metallic materials including the high specific strength and stiffness, excellent manufacturability and immunity to corrosion, etc.^{1–3} First developed for military aircraft applications in 1970s, advanced composites now play a crucial role in a broad range of current generation military aerospace systems, resulting in the weight saving of 10–60% over those based on metal design, with 20–30% being typical as achieved by the U.S. Air Force B2 bomber and recent F-22 raptor (24%). Commercial transport aviation

has also witnessed a significant increase in adoption of polymer composites during the past decades; the new Boeing 787 Dreamliner is made from 50% polymer composites by weight and more than 50% by volume. Furthermore, with the recent eager demand for faster, agiler, and more mobile ground vehicles in the U.S. military operations⁴ and the growing concern of cost-saving and fuel efficiency in civil vehicles, polymer composites have been finding rapidly growing applications in lightweight composite armors, load-carrying parts in ground vehicles, etc.

Yet, there continue to be barriers and challenges to the expanding exploitation of composites technology for primary transport structures such as the wing and fuselage in aircrafts and composite propulsion shaft in heavy duty ground vehicles. These

include the damage tolerance, fuel containment, lightning protection, repair and nondestructive inspection, modeling and failure prediction, cost-effective manufacturing, and so on.⁵ Beyond these, advanced composites with self-healing function are particularly attractive. For example, if an antenna of the space station was made of self-healing composites, it could be possible to save the huge maintenance cost associated with space walks and shuttle launches. To date, most research in advanced composites has been focused on further exploitation of the existing properties to satisfy the ever growing demands in aggressive structural applications; however, relatively less has been dedicated to the exploration of innovative material functions including damage self-repairing and stiffness/strength self-recovery to mimic the functionalities of biological bodies in nature.

In nature, the ability of biological bodies to heal (e.g., bleeding, blood clotting, tissue bruising, tree bark compartmentalization, etc.) has inspired several self-healing mechanisms that can be explored for use in engineering materials.⁶ Yet, the biological self-healing mechanisms are usually too complicated to be mimicked directly in engineering materials. In recent years, materials scientists and engineers have formulated several simplified material-healing concepts that offer the potential of restoring the mechanical performance of engineering materials.^{6–14} For lightweight structural polymer matrix composites (PMCs), two basic self-healing mechanisms to mimic mammal bleeding have been intensively studied in recent years, in which the self-healing chemistry is based on the living ring-opening metathesis polymerization (ROMP).¹⁵ The first self-healing system is based on the microencapsulation approach, in which the microcapsules containing the liquid healing agent (healant) and the polymeric resin containing the catalyst form the constitutive phases of the composite^{7,16–25}; the second is based on hollow microfibers containing healing agent.^{26–33} In principle, each self-healing strategy consists of a healant microcontainer (either microcapsule or hollow microfiber) and a dispersed catalyst inside the polymeric resin. Upon cracking, the wall of the microcontainers (typically with brittle waxy or glass walls) can be ruptured by the propagating crack front, resulting in the release of healant into the crack surfaces via capillary action. Subsequent ROMP of the healant under the initiation of the embedded catalyst heals the microcracks and prevents further crack growth. To date, the mostly studied self-healing system for PMCs is made up with dicyclopentadiene (DCPD, C₁₀H₁₂) as healing agent and Grubbs' catalyst. The synthesis and characterization of the Grubbs' catalysts have been extensively investigated.¹⁵ The DCPD/Grubbs' catalyst system carries a number of advantages such as a long shelf life, low-monomer viscosity and volatility, completion of polymerization in several minutes at ambient condition, low shrinkage upon polymerization, and formation of a tough and highly cross-linked crack filling material.^{7,10} In addition, the healing based on ROMP of DCPD and Grubbs' catalyst may form living poly-(DCPD) chain ends capable of continuously growing with the addition of more monomers. If a new monomer is supplied at the end of the chain, further ROMP can be triggered and the chain extends to make it possible to achieve multiple healings simply via replenishing the supply of the DCPD monomer.

To fulfill an ROMP-based self-healing composite, it is essential to develop a feasible healant encapsulation system capable of protecting either the healant or the catalyst, or both, making the selection and manufacturing of effective self-healing microcontainers the first step towards a successful application of this material concept. A suitable self-healing system should be (a) easily encapsulated and ruptured; (b) stable and reactive over the entire service life of the polymeric components under broad environmental conditions; (c) responsive quickly to heal damage once triggered; (d) low-cost and low-adverse impact on the original material properties.¹² By examining the current self-healing PMCs, it is found that the typical size of healant containers (either microcapsules or hollow microfibers) is up to hundreds of micrometers, much larger than that of the reinforcing microfibers in PMCs. Due to the stress concentration, the large healant containers in brittle matrix may yield spots of earlier failure of the composites. Also, large-sized microcapsules and hollow glass fibers could not be introduced into the ultrathin thin resin-rich interlayers (with the typical thickness of tens of micrometers) of fiber-reinforced PMCs to heal the dominative interfacial damage (e.g., delamination).

Therefore, in this study, we proposed a novel interfacial self-healing technique for PMCs based on healant-loaded core-shell nanofibers. A proof-of-concept hybrid multiscale self-healing PMC was processed via integration of coelectrospun core-shell DCPD/PAN nanofibers at laminate interfaces. Three-point bending test was used to evaluate the self-healing effect in such novel self-healing PMC after predamage failure. Scanning electron microscope (SEM) was utilized for fractographical analysis in exploring the healing mechanisms of the core-shell nanofibers at ply interfaces. In the rest of the article, introduction of the conceptual hybrid multiscale self-healing PMCs was given in "Concept of Nanofiber-Based Interface Toughening and Self-Healing Method for Fiber-Reinforced PMCs" Section. The experimental details on fabrication of core-shell nanofibers loaded with the healing agent and processing of the novel hybrid multiscale self-healing PMCs were described in "Experimental" Section. Reduction of the experimental data, exploration of the toughening and self-healing mechanisms, and comparison of the present work with those in reported in the literature were given in "Experimental Results and Interfacial Toughening and Self-Healing Mechanisms" Section. Consequently, conclusions of the present research were drawn in "Concluding Remarks" Section.

CONCEPT OF NANOFIBER-BASED INTERFACE TOUGHENING AND SELF-HEALING METHOD FOR FIBER-REINFORCED PMCS

In principle, the mechanical behavior of a PMC is a combined effect of the composite constituents (i.e., the reinforcing fibers and polymeric matrix), fiber/matrix interfacial properties, microstructure of the composite (e.g., fiber alignment, ply layout, fiber volume fraction, etc.), dominative failure modes, etc. Subjected to external loading, the failure process of a fiber-reinforced PMC laminate is typically a progressive avalanche consisting of microcrack nucleation, matrix cracking, fiber breakage, fiber and matrix debonding, delamination, and final catastrophic failure. The typical damage modes in a cross-ply

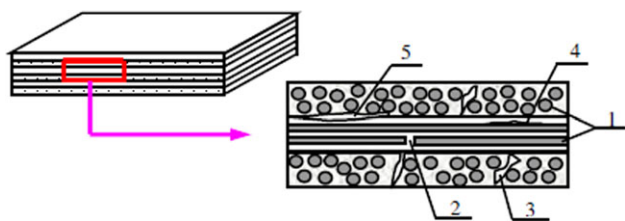


Figure 1. Schematic damage modes in a cross-ply polymer composite: (1) reinforcing fibers, (2) fiber breakage, (3) matrix cracking, (4) fiber/matrix debonding, and (5) delamination. [Color figure can be viewed in the online issue, which is available at wileyonlinelibrary.com.]

fiber-reinforced PMC laminate are illustrated in Figure 1. The actual failure process of a PMC is much more complicated, highly depending upon the types of load, fiber and ply architecture, and physical properties of the constituents, among others.

In reality, given a fiber/matrix combination, a pragmatic toughening technique adoptable to enhance the strength and toughness of a PMC needs to address and resolve one or several failure modes at an affordable cost. To date, several effective toughening techniques and concepts have been formulated and implemented in PMCs such as the free-edge delamination-suppression designs,³ laminate stitching,³⁴ modification of matrix resins via incorporation of rigid/rubbery micro and nanoparticles,^{35,36} controlled fiber debonding and fiber surface treat-

ment,³⁷ and interleaving.³⁸ Among these, the free-edge delamination-suppression concept (either edge reinforcement or edge modification) is rooted in altering the singular free-edge stresses near laminate edges,^{3,39,40} while interleaving is based on incorporating discrete thin interlayers of tough plastic resin, particulates, whiskers, or microfibers into the interlaminar regions and therefore enhances the interlaminar fracture toughness, especially in the cases of mode II shearing and impact. Recently, by comprehensively utilizing the advantages of the above interface toughening techniques and the progress in fabrication of continuous nanofibers, an innovative delamination suppression scheme for PMCs has been proposed on the basis of incorporation of discrete, ultrathin fibers at ply interfaces.^{41–43} The resulting hybrid multiscale PMC is illustrated in Figure 2, in which the ultrathin reinforcing fibers can be tough plastic polymer nanofibers produced by polymer-solution electrospinning,^{44–49} glass nanofibers⁵⁰ by melt electrospinning, or carbon nanofibers prepared via carbonization of as-electrospun polymer nanofiber precursor.^{51,52} Our recent experimental studies have indicated that electrospun polymer (PAN), glass (SiO₂), and carbon nanofibers can noticeably enhance the delamination toughness (20–50%) and interlaminar shear strength of PMC laminates in a wide range of loading rate,^{49,50–52} especially in the extension of fatigue life cycle of angle-ply PMCs.⁴⁹ The toughening mechanisms of these reinforcing nanofibers at the interfaces of PMCs include improvement of the interlaminar fracture toughness of PMCs and suppression of the singular stresses near laminate

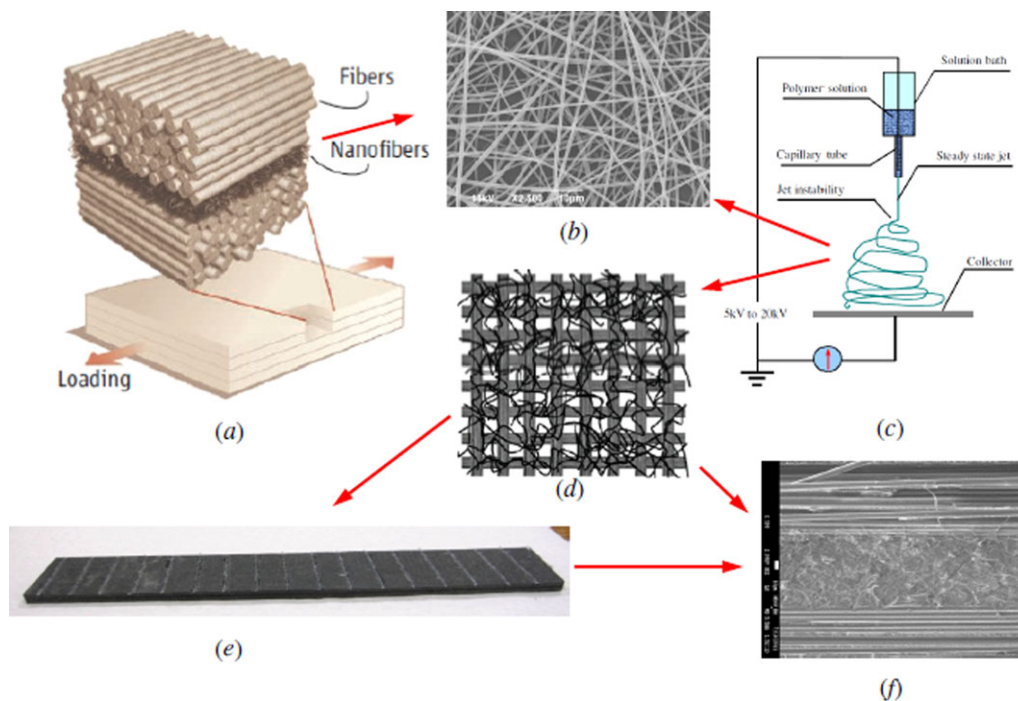


Figure 2. Hybrid multiscale PMC reinforced with electrospun continuous nanofibers at interfaces. (a) Schematic diagram of the conceptual PMC [41] (with the permission for use from AAAS), (b) nonwoven electrospun nanofibers, (c) schematic setup of electrospinning for fabrication of continuous nanofibers, (d) schematic woven fabric coated with nonwoven electrospun nanofibers, (e) hybrid multiscale PMC laminate produced by wet layup followed by VARTM technique, and (f) SEM micrograph of a nanofiber reinforced interlayer (cross-section of the hybrid multiscale PMC). [Color figure can be viewed in the online issue, which is available at wileyonlinelibrary.com.]

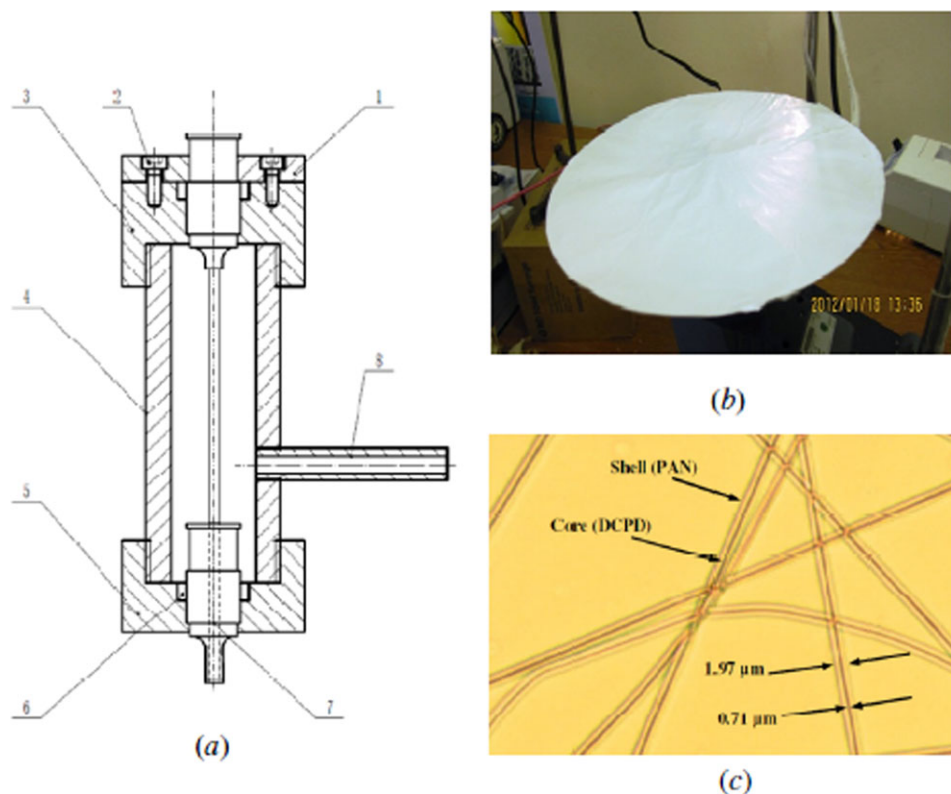


Figure 3. (a) Schematic coaxial spinneret: (1): pressing plate, (2) tightening screws, (3) upper nut, (4) master tube, (5) lower nut, (6) seal rube ring, (7) outer nozzle coaxially assembled with the inner nozzle (upper), and (8) outer tube; (b) core-shell DCPD/PAN nanofiber mat (collected on a rotary disk-like collector) by coelectrospinning; (c) optical micrograph of typical core-shell DCPD/PAN nanofibers. [Color figure can be viewed in the online issue, which is available at wileyonlinelibrary.com.]

free-edges since the entangled nanofibers at interfaces behave much like the hooks and loops in Velcro.⁴¹ The main advantages of this interface toughening technique include the low-weight penalty (<1% in volume fraction), low nanofiber content, and low impact to the processing and global properties of the PMCs (e.g., specific stiffness, volume fraction of the reinforcing fibers, etc.). Thus, this toughening technique could be easily integrated into the fabrication process of conventional PMCs. Yet, similar to other interface toughening techniques, this interface toughening scheme does not carry any self-repairing function. In fact, the mechanical properties of PMCs reinforced with such continuous nanofibers at ply surfaces will still irreversibly degrade with time. Thus, a desirable interface toughening strategy for advanced PMCs is expected being capable of both interfacial toughening and self-healing at low cost and tailorable ultrathin size.

In this study, in order to introduce the innovative self-healing function into the weak interfaces of fiber-reinforced structural PMCs, we produced novel liquid healant-loaded core-shell nanofibers by the low-cost coelectrospinning technique.^{53–55} These nonwoven core-shell nanofibers were incorporated at the ply interfaces of PMCs during laminate layup (Figure 2). Similar to processing of the hybrid multiscale PMCs aforementioned, after curing, the healant-loaded core-shell nanofibers could be entangled into the resin-rich interlayers (with the thickness of tens of micrometers) between the neighboring plies

to form the ultrathin toughening and self-healing interlayers. When interfacial failure starts in such self-healing PMCs subjected to external loading, before nanofiber scission, these core-shell nanofibers entangled at ply interfaces are expected to function as toughening nanofibers via nanofiber debonding, bridging, and plastic deformation.^{41,49} Furthermore, once nanofiber scission happens due to crack-opening, fiber stretching and pull-out induced breakage, the liquid healant stored in the core-shell nanofiber network would autonomically release at crack fronts under the action of capillary force and then heal the cracks, resulting in interfacial self-healing effect, and stiffness/strength recovery.

EXPERIMENTAL

Coelectrospinning of Healant-Loaded Core-Shell Nanofibers

The chemicals of PAN powder ($M_w = 150,000$ g/mol), *N,N*-dimethylformamide (DMF, 99%), DCPD, and Grubbs' catalyst were purchased from Sigma-Aldrich Co. (St. Louis, MO) without further purification and modification. For coelectrospinning, a solution of 10 Wt. % PAN in DMF was prepared to generate the PAN shell material and a solution of 10 wt % DCPD in DMF was prepared to generate the liquid DCPD core as healing agent. The well-electrospinning PAN/DMF solution was prepared by dissolving the PAN powder in DMF at 80°C for 6 h with magnetic stirring. The DCPD/DMF solution was

made by dissolving the liquid DCPD in DMF at room temperature. During the coelectrospinning process, a laboratory-made coaxial spinneret as illustrated in Figure 3(a) was used, which is made up with two coaxially assembled nozzles. The outer nozzle has its inner diameter of 0.97 mm; the inner one carries its outer and inner diameters as 0.71 mm and 0.48 mm, respectively. The PAN/DMF and DCPD/DMF solutions were placed in two 10-mL syringes and connected to the outer and inner nozzles of the coaxial spinneret, respectively. The flow rates of the solutions in the outer and inner nozzles were controlled via two digital syringe pumps (Fisher Scientific Inc., Pittsburgh, PA) such that the flow rates of the PAN/DMF and DCPD/DMF solutions were 1.5 mL/h and 1.0 mL/h, respectively. A distance of ~ 25 cm was fixed between the spinneret outlet and the nanofiber collector, which was a rotary disk-like aluminum plate electrically grounded. A high DC voltage ~ 18 kV was applied between the spinneret outlet and the nanofiber collector via a positive high-voltage DC power supply (Gamma High Voltage Research, Inc., Ormond Beach, FL). A stable coelectrospinning process could be secured via tuning the process parameters (e.g., applied DC voltage, flow rates, and distance between the nozzle outlet and nanofiber collector) around the values above. In addition, an optical microscope (IX 71 Olympus) was utilized to characterize the as-coelectrospun core-shell nanofibers. Figure 3(c) shows the typical continuous core-shell nanofibers loaded with liquid DCPD as the core material. The thickness of the nonwoven healant-loaded core-shell nanofiber mat can be altered by adjusting the nanofiber collection time. In this study, the nanofiber collection time was fixed at 40 min for maximization of the interfacial toughening effect according to our recent study.⁴⁹

Processing of Hybrid Multiscale Self-Healing PMCs and Self-Healing Characterization

Commercially available UD carbon-fiber/epoxy prepregs⁴⁹ and woven carbon fabric/epoxy^{50–52} have been investigated for producing hybrid multiscale carbon-fiber/epoxy composites reinforced with as-electrospun PAN nanofibers and carbonized as-electrospun PAN nanofibers at interfaces in our recent studies. The former was based on prepreg layup using vacuum-bag compressive molding with the aid of a hot-press; the latter was based on vacuum-assisted resin transfer molding (VARTM) technique. In this study, wet layup followed by VARTM technique was used to process the novel hybrid multiscale self-healing PMCs, in which wet layup method would ensure the uniform wetting of the nano/microfiber fabrics into resin.

During the process, Epon 862 epoxy resin and Epicure 3234 curing agent were selected as the polymeric matrix for processing the novel PMC in this work.⁵⁶ This resin system was purchased from Miller-Stephenson Chemical Company, Inc. (Morton Grove, IL). The mix ratio of Epon 862 and Epicure 3234 was 100: 14 by weight according to the manufacturer's data sheet; a tiny quantity of Grubbs' catalyst (~ 0.1 g) was added into the resin (~ 20 g) during mixture to produce the composite panel. The reinforcing UD carbon fabrics (9.0 oz/yd²) and cross-woven carbon fabrics (5.7 oz/yd²) were purchased from Fibre Glaz Development Corp. (Brookville, OH). An eight-ply quasi-isotropic composite laminate with a $[0^\circ/\pm 45^\circ/90^\circ]_S$ stacking sequence was manufactured, in which the 0° and 90° plies

were based on the UD carbon fabrics while the $+45^\circ$ and -45° plies were based on the cross-woven carbon fabrics. The core-shell self-healing nanofiber mats were placed at the interfaces of $0^\circ/45^\circ$ and $45^\circ/90^\circ$, respectively, where out-of-plane interfacial shear failure (delamination) was expected due to the large free-edge stresses based on a semi-analytic model.^{49,57} During the VARTM process, the vacuum pressure of 27 mmHg had been maintained at the initial curing stage at room temperature for 24 h. The obtained composite panel had been further post-cured in an oven (at 100°C for 1 h) before the mechanical test for self-healing evaluation.

For the purpose of the mechanical characterization of the self-healing specimens, the PMC specimens with dimensions: ~ 100 mm \times 20 mm \times 2.35 mm were cut from the above post-cured PMC laminate ($5'' \times 5'' \times 0.1''$) using a diamond-tipped rotary saw installed with a water-cooling system. Edges of the machined specimens were polished manually using sandpaper to avoid possible predamage during the test. Three-point bending test (ASTM-D790) was selected to characterize the flexural stiffness of the novel hybrid multiscale PMC specimens reinforced with self-healing core-shell nanofibers at interfaces on an Instron machine. Figure 4 shows the three-point bending test setup, in which the span between the two supporting pins was fixed at 75 mm. All the mechanical tests were performed at room temperature with a displacement-control mode such that the loading rate of 5 mm/min was applied. In the preliminary study of this research, three specimens were prepared and tested successfully for evaluating the self-healing effect of healant-loaded core-shell nanofibers in the flexural stiffness recovery after first interlaminar cracking happened.

With the three-point bending test setup (Figure 4), predamage test to trigger interlaminar cracking was first performed by loading the self-healing composite specimens at a constant crosshead speed of 5 mm/min until first interlaminar cracking happened, corresponding to an abrupt drop in the force-displacement diagram recorded by the MTS machine. Then, the test was stopped and the specimen was unloaded immediately and removed from the testing frame. After 2 h, all the predamaged specimens were post-tested at room temperature using the same testing procedure and control parameters above. As a result, two load-displacement curves can be gained and recorded for each specimen, corresponding to the pre- and post-damage tests, respectively. Typical failed portions of the specimens were sampled and coated with an ultrathin carbon (a few nanometers by estimation) by using a sputter. These samples were used for fractographical analysis and exploration of the potential interfacial toughening and self-healing mechanisms of the core-shell nanofibers by using a JEOL JSM-7600F analytical high-resolution field-emission SEM.

EXPERIMENTAL RESULTS AND INTERFACIAL TOUGHENING AND SELF-HEALING MECHANISMS

Herein, we introduce the recovery ratio of the initial flexural stiffness of the self-healing PMC laminates for quantitative evaluation of the healing efficiency of the interfacial self-healing method developed in this study. The stiffness recovery ratio can be defined as

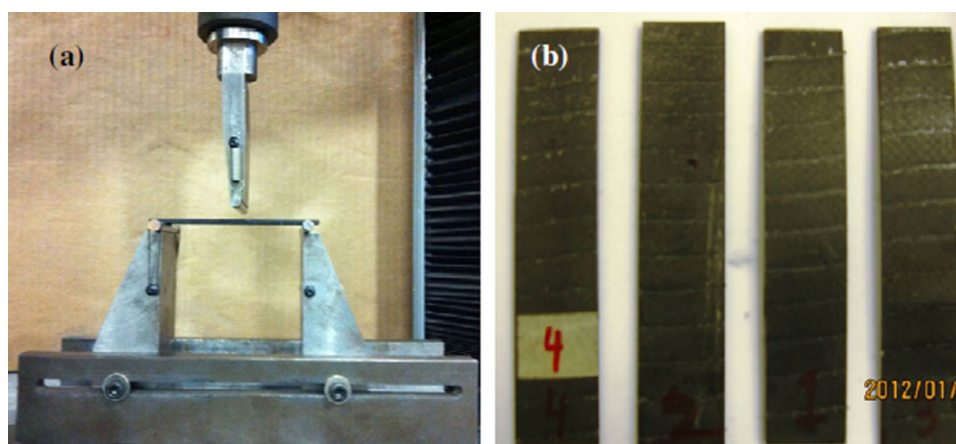


Figure 4. (a) Three-point bending test setup with the span 75 mm between the two supporting pins; (b) three-point bending specimens with the dimensions: $\sim 100 \text{ mm} \times 20 \text{ mm} \times 2.35 \text{ mm}$. [Color figure can be viewed in the online issue, which is available at wileyonlinelibrary.com.]

$$\text{Stiffness recovery ratio} = \frac{\text{Healed flexural stiffness}}{\text{Initial flexural stiffness}} \times 100\% \quad (1)$$

In the above, the initial flexural stiffness was the flexural stiffness of a virgin self-healing PMC specimen subjected to three-point bending load, and the healed flexural stiffness is the flexural stiffness of a predamaged specimen after healing for one hour. As a matter of fact, predamage failure of an angle-ply fiber-reinforced PMC laminate under three-point bending was due mainly to delamination failure. Thus, breakage of the healant-loaded core-shell nanofibers at interfaces would release liquid DCPD, which polymerized and healed the interfacial cracks once being triggered by the Grubbs' catalyst in resin. The experimental results of the initial flexural stiffness, residual flexural stiffness after predamage failure, healed flexural stiffness, and the stiffness recovery ratio were tabulated in Table I. The stiffness recovery ratio of the self-healing PMC specimens is up to 70 to 100%, and the healed flexural stiffness is up to 150 to 300% of the flexural stiffness of the PMC specimens after predamage failure. It needs to be mentioned that in this preliminary study, the duration for self-healing (the time interval between the predamage test and post-damage test) of the self-healing PMC was $\sim 2 \text{ h}$. Thus, the study indicates that liquid healant-loaded core-shell nanofibers at ply interface behaved excellent self-healing effect on the flexural stiffness of the PMC laminates.

Figure 5 shows the load-displacement curves of two typical self-healing specimens subjected to pre and post-damage three-point bending loads, respectively. From Figure 5, it can be founded

that the predamage load-displacement curves [the solid curves in Figure 5(a,b)] corresponding to the predamage failure are similar to those of common thermosetting carbon-fiber/epoxy PMCs. However, after self-healing, the post-damage load-displacement curves [the dashed curves in Figure 5(a,b)] exhibit some interesting features relevant to the self-healing process. For instance, the results of post-damage tests indicated the nearly complete recovery of the initial flexural stiffness, *i.e.*, the specimens after self-healing carried the approximately same slope of the load-displacement curves as the predamage tests; the healed flexural stiffness was much higher than the residual one after predamage test. Furthermore, the healed flexural strength as showed in Figure 5(a) could reach the flexural strength of the virgin specimen, which is double the residual flexural strength of the predamaged specimen; in Figure 5(b), the healed flexural strength is $\sim 30\%$ higher than the residual flexural strength of the predamaged specimen though the healed flexural strength is lower than that of the virgin specimen. The latter might be the result of breakage of the reinforcing carbon fibers in the 0° -plies due to the large deflection at the moment of predamage failure, *i.e.*, incurable reinforcing-fiber failure. Moreover, Figure 5(b) also indicates that after self-healing, the healed PMC specimen exhibited ductile behavior that could be correlated to the plastic behavior of polymerized DCPD at the healed interfaces. Such interfacial plastic behavior expects to substantially enhance the interlaminar fracture toughness of the self-healing PMC laminates.

Moreover, SEM-based fractographical analysis was performed to explore the potential interfacial toughening and self-healing

Table I. Experimental Results of Three-Point Bending Tests and Healing Efficiency of the Self-Healing PMC Specimens in Terms of Stiffness Recovery Ratio

Sample no.	Initial flexural stiffness (E_0) (kN/m)	Flexural stiffness after predamage failure (E_f) (kN/m)	Flexural stiffness after healing (E_h) (kN/m)	Stiffness recovery ratio (%)
1	163.9	61.2	159.0	97.0
2	144.8	74.5	99.0	68.3
3	145.5	46.3	150.5	103.4

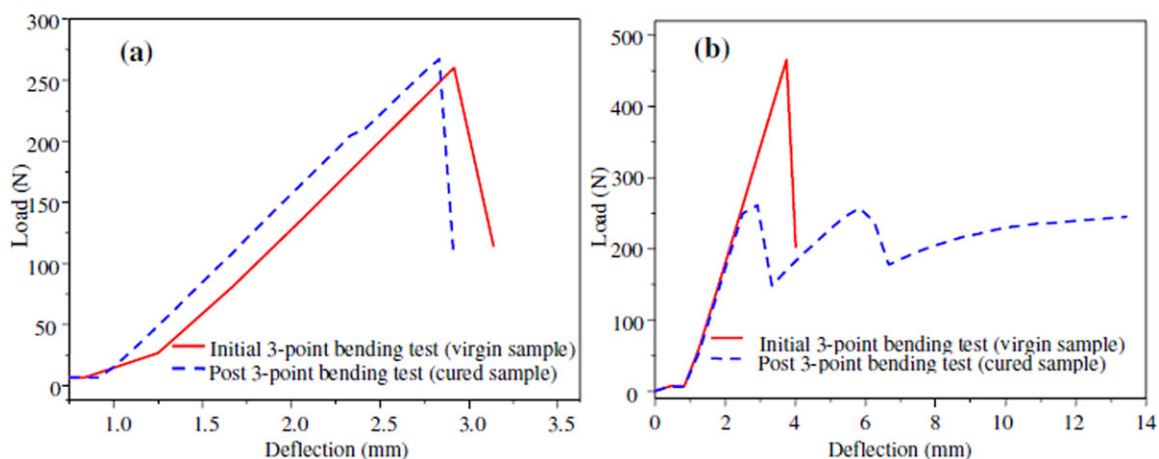


Figure 5. Comparative load-displacement curves of two typical hybrid multiscale self-healing PMC specimens subjected to three-point bending loads. [Color figure can be viewed in the online issue, which is available at wileyonlinelibrary.com.]

mechanisms of the unique core-shell nanofibers at ply interfaces. For the purpose of estimating the thickness of core-shell nanofiber interlayers after curing, Figure 6 was taken to show the cross-sectional SEM-view of a similar UD carbon-fiber reinforced PMC with electrospun nanofibers at ply interfaces; the sample was prepared using the same process parameters as the present self-healing PMC. The thickness of the nanofiber interlayer is estimated $\sim 80 \mu\text{m}$. With the consideration of the thickness of resin-rich interlayer in PMCs even below this value (after eliminating the nanofiber contribution), the conventional self-healing techniques based on microcapsulation and hollow glass fibers as reported in the literature are unable to be used for such interfacial self-healing. However, the present core-shell nanofibers with the diameter ranging from hundreds of nanometer to a couple of micrometers can function to toughen and heal such thin interlayers in PMCs.

In addition, Figure 7 shows the typical fracture surfaces of the self-healing PMC after three-point bending failure. It can be clearly observed that when the core-shell nanofibers were scissored at interfaces due to interfacial crack initiation and opening, the liquid DCPD released at crack surfaces. Once the releasing DCPD touched the Grubb's catalyst in the matrix resin, the liquid DCPD polymerized and solidified instantaneously to seal and bind the crack surfaces, similar to discrete stitching pins. Figure 7(a,b) also show the typical core-shell nanofiber networks containing liquid DCPD healant at ply surfaces, where the circled regions indicate the spots of healant release out of the ruptured core-shell nanofibers and solidification. Figure 7(c,d) show the zoomed regions where the DCPD healant was delivered and polymerized at interfaces after the predamage test, and finally refractured to form the newborn crack surfaces during the post three-point bending test. The surface morphology of the newborn crack surfaces including matrix hackles and scalloped features indicates the existence of DCPD-related ductile interfacial failure during the post three-point bending test as expected. Additional features associated with the healant release from the core-shell fibers on the scale of individual fibers are shown in the SEM micrographs in Figure 8. It can be found that under pressure DCPD was

squeezed out of the core, and Figure 8(c) shows that squeezing even resulted in a crack in the shell.

Furthermore, as shown in Figure 9, the healant-loaded core-shell nanofibers can also function to toughen the polymer matrix simultaneously via nanofiber bridging, pull-out, breakage, etc., similar to the toughening mechanisms of solid nanofibers produced by electrospinning as explored in our recent studies of interfacial toughening.^{49–52}

In addition, by comparison with recently developed self-healing techniques such as those based on micro/nanocapsules and hollow glass microfibers, the present self-healing technique has its merits. First, encapsulation of the healing agent to form core-shell nanofibers is based on the low-cost coelectrospinning technique. This process can be conveniently tailored via adjusting the process and material parameters for well uniform fiber diameter and optimized thickness of the nanofiber mats. This technique can also be scaled up for stable and mass production. Note also, that in addition to coelectrospinning, we have

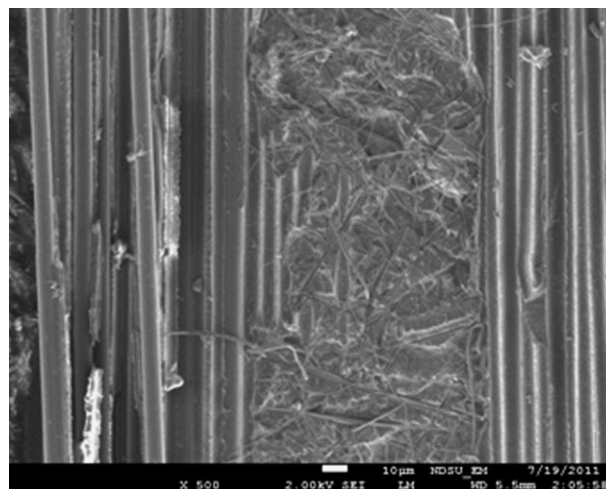


Figure 6. SEM micrograph of the cross-sectional area of a nanofiber interlayer in a UD carbon-fiber reinforced PMC.

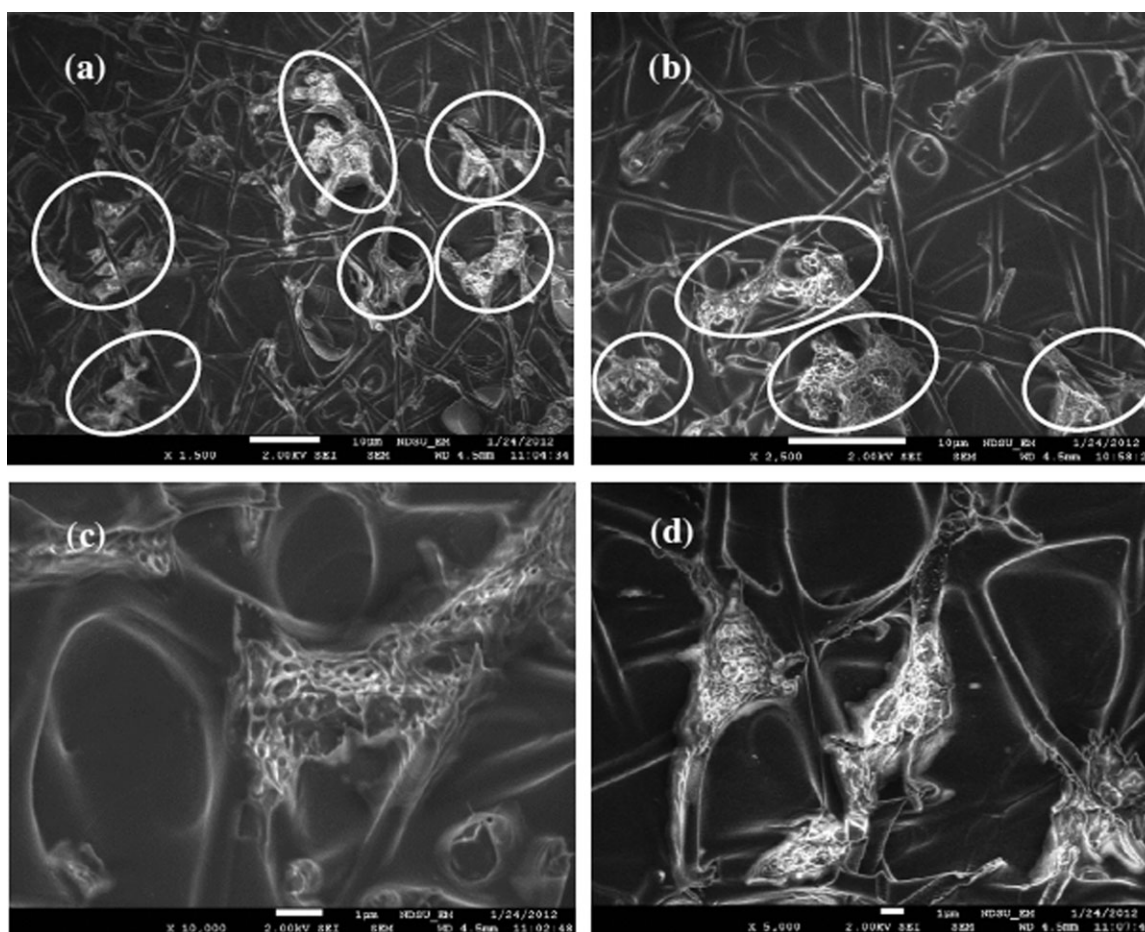


Figure 7. SEM micrographs of failed surfaces of the hybrid multiscale self-healing PMC after three-point bending test (interfacial self-healing mechanisms). (a,b) Core-shell nanofiber networks (circled spots are the regions with autonomously released DCPD after pre-damage failure); (c,d) Delivery of healing-agent at core-shell nanofiber breakages due to interfacial and plastic failure of healed spots after post three-point bending test.

recently developed several innovative cost-effective techniques for encapsulating healing agents into nanofibers/nanotubes via emulsion electrospinning, solution blowing, and self-sustained diffusion.⁵⁵ Second, the present core-shell nanofibers carried the diameters nearly two orders smaller than those based on microcapsules and hollow microfibers as reported recently in the literature,^{7,16–18,26–28} thus the present self-healing technique can be utilized specifically for localized interfacial toughening and self-healing within a few micrometers, particularly applicable to advanced aerospace and aeronautical PMCs which intrinsically bear the weak resin-rich interlayers with the thickness of tens of micrometers as demonstrated in this study. For these PMCs, interfacial toughening and self-healing based on a tiny quantity of continuous core-shell nanofibers at interfaces will not result in an obvious weight penalty and decrease of the superior specific stiffness and strength. Third, due to their continuity and deposition throughout the interfaces, these core-shell nanofibers can be easily scissored at any location of the interfaces once interfacial cracking (delamination) happens. In contrast, nanocapsules are difficult to rupture by crack fronts; also, the low volume of healant stored in localized nanocapsules, difficult control of fabrication (generally in a wide range of size distribu-

tion) and requirement of a uniform mixture may project some additional limitations on use of micro/nanocapsules in self-healing of PMC laminates. Lastly, continuous core-shell nanofiber mats can be easily sandwiched between prepregs or fiber fabrics, thus the present toughening and self-healing technique can be conveniently merged into the process of traditional PMCs manufacturing based on either prepreg layup or wet layup followed by VARM technique. In short, this study opens up an innovative route for efficient interfacial toughening and self-healing techniques for advanced PMCs and other advance composites. Nevertheless, as a new cutting-edge self-healing technique, several outstanding materials science and technological issues still need resolving such as choice of proper shell material, controlled deposition of catalyst at interfaces, effect of fiber size and core/shell aspect ratio, and effect of temperature, loading rate, failure mode, etc.

CONCLUSIONS

In this study, a new type of hybrid multiscale high-strength carbon-fiber/epoxy composites reinforced with core-shell toughening and self-healing nanofibers at interfaces has been proposed

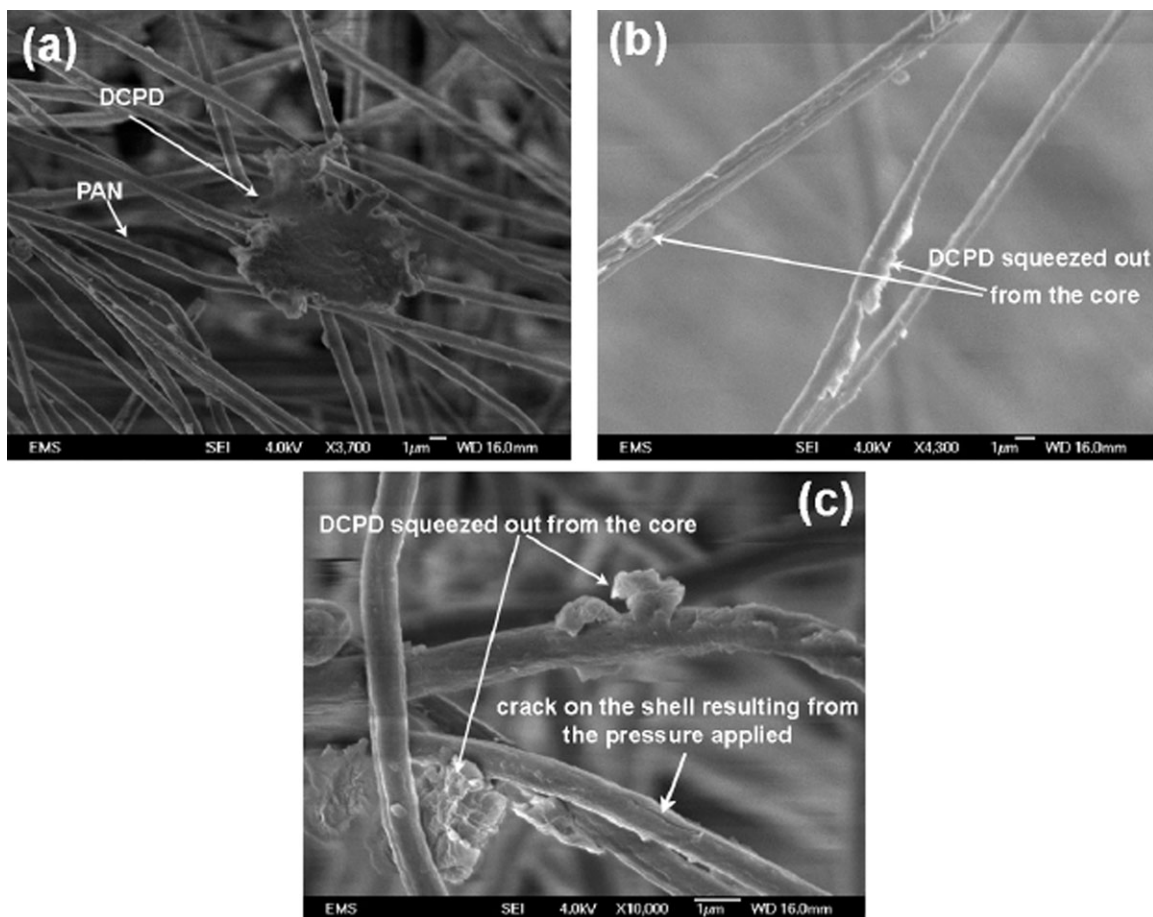


Figure 8. SEM images of squeezed core-shell DCPD-PAN nanofibers. (a,b) show several characteristic morphologies of DCPD release from the core; (c) shows a crack in the shell.

and successfully fabricated and characterized. The unique hea-lant-loaded ultrathin core-shell nanofibers were fabricated by means of the low-cost, top-down coelectrospinning technique. The present interfacial toughening and self-healing technique

has extended the functionality of the recently developed nano-fiber-based interfacial toughening technique for PMC laminates, where suppression of interfacial fracture (delamination) is still a challenge. The present technique has a very low weight penalty

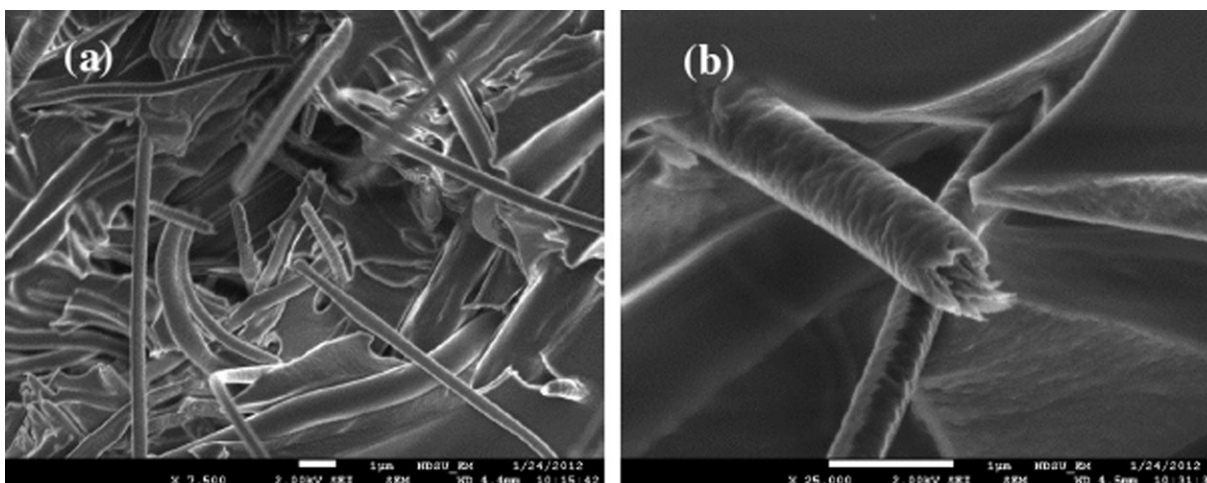


Figure 9. SEM micrographs of failed surfaces of the hybrid multiscale self-healing PMC after post-three-point bending test (interfacial toughening mechanisms). (a) Core-shell nanofiber pull-out and bridging; (b) core-shell nanofiber pull-out, plastic necking, and breakage.

(<1% in volume fraction), very low nanofiber content, and very low impact to the processing and global specific properties of the PMCs. Thus, this novel interfacial toughening and self-healing technique has a promising future and is expected very useful for developing high-strength, high-toughness, self-healing lightweight PMCs for advanced structural applications in aerospace, aeronautical, ground vehicles, sports utilities, and so on.

ACKNOWLEDGMENTS

The financial support of the research at NDSU by the ND NASA EPSCoR (NASA Grant # NNX07AK91A, seed grant: 43500-2490-FAR018640) and NDSU Development Foundation (XFW) was gratefully acknowledged. Thanks go to Professor Chunwei Sun of the Department of Pharmacy at NDSU for kind assistance with the optical microscopy of the core-shell nanofibers.

REFERENCES

1. Tsai, S. W. *Compos. Sci. Technol.* **2005**, *65*, 2295.
2. Chou, T. W. *Microstructural Design of Fiber Composites*; Cambridge: Cambridge University Press, **1992**.
3. Jones, R. M. *Mechanics of Composite Materials*, 2nd ed.; Philadelphia: Taylor and Francis, **1999**.
4. Lane, R. A. *AMPTIC* **2005**, *9*, 3.
5. Tenney, D.; Pipes, R. B. *Advanced Composites Development for Aerospace Applications*. Presented in The Seventh Japan International SAMPE Symposium and Exhibition, Tokyo, Japan, November 13, **2001**.
6. Trask, R. S.; Williams, H. R.; Bond, I. P. *Bioinsp. Biomim.* **2007**, *2*, 1.
7. White, S. R.; Sottos, N. R.; Geubelle, P. H.; Moore, J. S.; Kessler, M. R.; Sriram, S. R.; Brown, E. N.; Viswanathan, S. *Nature* **2001**, *409*, 794.
8. Wool, R. P. *Nature* **2001**, *409*, 773.
9. Sottos, N.; White, S.; Bond, I. *J. R. Soc. Interface* **2007**, *4*, 347.
10. van der Zwaag, S. *Self-Healing Materials: An Alternative Approach to 20 Centuries of Materials Science*; Springer: Heidelberg, **2007**.
11. Shchukin, D. G.; Möhwald, H. *Small* **2007**, *3*, 926.
12. Wu, D. Y.; Meure, S.; Solomon, D. *Prog. Polym. Sci.* **2008**, *33*, 479.
13. Blaiszik, B. J.; Kramer, S. L. B.; Olugebefola, S. C.; Moore, J. S.; Sottos, N. R.; White, S. R. *Annu. Rev. Mater. Res.* **2010**, *40*, 179.
14. Murphy, E. B.; Wudl, F. *Prog. Polym. Sci.* **2010**, *35*, 223.
15. Bielawski, C. W.; Grubbs, R. H. *Prog. Polym. Sci.* **2007**, *32*, 1.
16. Kessler, M. R.; Sottos, N. R.; White, S. R. *Compos. A* **2003**, *34*, 743.
17. Brown, E. N.; White, S. R.; Sottos, N. R. *Compos. Sci. Technol.* **2005**, *65*, 2466.
18. Brown, E. N.; White, S. R.; Sottos, N. R. *Compos. Sci. Technol.* **2005**, *65*, 2474.
19. Rule, J. D.; Sottos, N. R.; White, S. R. *Polymer* **2007**, *48*, 3520.
20. Jones, A. S.; Rule, J. D.; Moore, J. S.; Sottos, N.; White, S. R. *J. R. Soc. Interface* **2007**, *4*, 395.
21. Yin, T.; Rong, M. Z.; Zhang, M. Q.; Yang, G. C. *Compos. Sci. Technol.* **2007**, *67*, 201.
22. Blaiszik, B. J.; Sottos, N. R.; White, S. R. *Compos. Sci. Technol.* **2008**, *68*, 978.
23. Patel, A. J.; Sottos, N. R.; Wetzel, E. D.; White, S. R. *Compos. A* **2010**, *41*, 360.
24. Cho, S. H.; White, S. R.; Braun, P. V. *Adv. Mater.* **2009**, *21*, 645.
25. Huang, M. X.; Yang, J. L. *J. Mater. Chem.* **2011**, *21*, 11123.
26. Bleay, S. M.; Loader, C. B.; Hawyes, V. J.; Humberstone, L.; Curtis, P. T. *Compos. A* **2001**, *32*, 1767.
27. Pang, J. W. C.; Bond, I. P. *Compos. A* **2005**, *36*, 183.
28. Pang, J. W. C.; Bond, I. P. *Compos. Sci. Technol.* **2005**, *65*, 1791.
29. Hayes, S. A.; Jones, F. R.; Marshiya, K.; Zhang, W. *Compos. A* **2007**, *38*, 1116.
30. Trask, R. S.; Williams, G. J.; Bond, I. P. *J. R. Soc. Interface* **2007**, *4*, 363.
31. Hansen, C. J.; Wu, W.; Toohey, K. S.; Sottos, N. R.; White, S. R.; Lewis, J. A. *Adv. Mater.* **2009**, *21*, 4143.
32. Park, J. H.; Braun, P. V. *Adv. Mater.* **2010**, *22*, 496.
33. Olugebefola, S. C.; Aragón, A. M.; Hansen, C. J.; Hamilton, A. R.; Kozola, B. D.; Wu, W.; Geubelle, P. H.; Lewis, J. A.; Sottos, N. R.; White, S. R. *J. Compos. Mater.* **2010**, *44*, 2587.
34. Dransfield, K.; Baillie, C.; Mai, Y. W. *Compos. Sci. Technol.* **1994**, *50*, 305.
35. Garg, A. C.; Mai, Y. W. *Compos. Sci. Technol.* **1988**, *31*, 179.
36. Low, I. M.; Mai, Y. M. In *Handbook of Ceramics and Composites*; Cheremisinoff, N. P., Eds.; **1990**; Vol. 2, pp 105–150.
37. Kim, J. K.; Mai, Y. W. *Compos. Sci. Technol.* **1991**, *41*, 333.
38. Carlsson, L. A.; Aksoy, A. *Int. J. Fracture* **1991**, *52*, 67.
39. Pipes, R. B.; Pagano, N. J. *J. Compos. Mater.* **1970**, *4*, 538.
40. Pagano, N. J. *J. Compos. Mater.* **1974**, *8*, 65.
41. Dzenis, Y. *Science* **2008**, *319*, 419.
42. Dzenis, Y. A.; Reneker, D. H. U. S. Pat. 6,265,333 (**2001**).
43. Doshi, J.; Reneker, D. H. *J. Electrostat.* **1995**, *35*, 151.
44. Reneker, D. H.; Chun, I. *Nanotechnology* **1996**, *7*, 216.
45. Dzenis, Y. *Science* **2004**, *304*, 1917.
46. Reneker, D. H.; Yarin, A. L.; Zussman, E.; Xu, H. *Adv. Appl. Mech.* **2007**, *41*, 43.
47. Reneker, D. H.; Yarin, A. L. *Polymer* **2008**, *49*, 2387.
48. Greiner, A.; Wendorff, J. H. *Angew. Chem. Int. Ed.* **2007**, *46*, 5670.
49. Wu, X. F. *Fracture of Advanced Composites with Nanostructured Interfaces: Fabrication, Characterization and Modeling*; VDM Verlag: Germany, **2009**.

50. Chen, Q.; Zhang, L. F.; Yoon, M. K.; Wu, X. F.; Arefin, R. H.; Fong, H. *J. Appl. Polym. Sci.* **2012**, *124*, 444.
51. Chen, Q.; Zhang, L. F.; Rahman, A.; Zhou, Z. P.; Wu, X. F.; Fong, H. *Compos. A* **2011**, *42*, 2036.
52. Chen, Q.; Zhang, L. F.; Zhao, Y.; Wu, X. F.; Fong, H. *Compos. B* **2012**, *43*, 309.
53. Sun, Z.; Zussman, E.; Yarin, A. L.; Wendorff, J. H.; Greiner, A. *Adv. Mat.* **2003**, *15*, 1929.
54. Yarin, A. L. *Polym. Adv. Technol.* **2011**, *22*, 310.
55. Sinha-Ray, S.; Pelot, D. D.; Zhou, Z. P.; Rahman, A.; Wu, X. F.; Yarin, A. L. *J. Mater. Chem.* **2012**, *22*, 9138.
56. Rahman, A. Fabrication and Mechanical Characterization of Novel Hybrid Carbon-Fiber/Epoxy Composites Reinforced with Toughening/Self-Repairing Nanofibers at Interfaces. M.S. Thesis, North Dakota State University, ND, USA, **2012**.
57. Wu, X. F.; Dzenis, Y. A. *Compos. Struct.* **2005**, *70*, 100.